*International Journal of Optoelectronics*, 1994, volume 9, number 6, pages 477–487

INVITED PAPER

# Guided wave optical switch architectures. Part 1. Space switching

D. K. HUNTER and I. ANDONOVIC

*Guided wave optical switching has been in existence for well over a decade and, at present, several architectures exist that could become candidates for use in optical systems. This paper will review optical space switching architectures, highlighting their performance parameters. Issues peculiar to optical implementation such as crosstalk, waveguide interface losses and attenuation will be considered. A similar treatment for optical time division switching will be presented in an accompanying paper.*

## 1. Introduction

Optical switching, as the name implies, involves the switching of optical signals, rather than electrical signals as in conventional electronic systems. One of the driving forces behind its development is that the signals to be switched can be at a much higher bit rate than with electronics. This is due to the EMI and pin out problems that plague large high-speed electronic systems.

Two types of guided wave optical switching systems can be identified. The first is a hybrid approach in which optical signals are switched, but the switches are controlled electronically. With this approach, the use of electrical control signals implies that the routeing will be carried out electronically. As such, the speed of the electronic switch control signals can be much less than the bit rate of the optical signals being switched. Nevertheless, factors such as clock skew and RC time constants limit the speed at which the electronics can operate, although this should not be a problem in many real applications where very high-speed reconfiguration rates are not required. The second approach is all-optical switching. Here, not only are signals switched optically but the switches are also controlled optically.

Received 24 March 1995.

*Authors' address:* University of Strathclyde, Department of Electronic and Electrical Engineering, Optoelectronics Division, 204 George Street, Glasgow G1 1XW, U.K. Tel: +(44)141 552 4400 Extn 2011; Fax: +(44) 141 552 2487; e-mail: d.k.hunter@uk.ac.strath.

The processing necessary to calculate the switch settings is optical. This potentially overcomes the problems associated with the hybrid approach. However, such systems will not become practical until far into the future and hence are not considered here.

This paper will confine itself to a description of hybrid guided-wave optical switching since it represents the most mature technology to date. Furthermore, the paper will concentrate on space-switch architecture, fabrics which set up connections between different circuits by setting switching devices or crosspoints. The review will highlight a number of switch types, emphasizing their disadvantages and performance parameters. There is a vast literature on the theory of these architectures, and only architectures that are amenable to optical implementation will be discussed. Issues peculiar to photonics implementations, e.g. crosstalk, interfacing, crossovers and attenuation, will be considered.

## 2. Switch model

Most architectures are realized with a regular array of switches called crosspoints. In the case of photonics these crosspoints take the form of $2 \times 2$ switches, which are most readily implemented with directional coupler switches (figure 1), or one of its variants [1]. These switches are the basic building block and may also be used as $1 \times 2$ or $2 \times 1$ switches by leaving an input or an output unused. Most space switch banks are organized

0952-5432/94 $10.00 

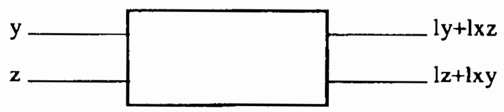


**Figure 1. Schematic of a guided-wave optical directional coupler switch (l = loss of switch; x = crosstalk).**

in stages, each state consisting of a column of switches. In each stage, except for the last one, each switch output is connected to a switch input on the next stage. The inputs of the first-stage switches form the input terminals of the architecture, and the outputs of the final-stage switches form the output terminals. An architecture is said to be blocking if there is one or more set of connections between different inputs and outputs that it cannot realize; i.e. it is not always possible to set up a new call between a pair of free input and output terminals. There are also non-blocking networks; strict sense non-blocking where there will always be at least one free route through the network for a new call, where the call may be set up without rerouteing the existing calls; wide sense non-blocking, where some rule must be used to decide what route to choose when activating a new call; and rearrangeably non-blocking networks, where new calls can always be accommodated but it may be necessary to re-route existing calls through the network.

Before discussing the architectures, some definitions must be introduced. The crosstalk (in dB) of a single directional coupler switch is represented by $X$ and its loss by $L$(dB). $X$ is always negative. The loss at each connection between an optical fibre and a waveguide, which are realized in an integrated optic geometry on a suitable substrate, is $W$(dB). SXR is the signal-to-crosstalk ratio of the whole switching network while the total insertion loss is $A$. If the signal enters the switch network, and passes through $K$ switches, the resulting SXR is approximately:

$$\mathrm{SXR} = -X - 10\log_{10} K(\mathrm{dB}) \qquad (1)$$

Throughout the paper two sets of values for $X$, $L$ and $W$ are used in calculations. The 'best case' values represent the best device reported [1] $X = -35$ dB, $L = 0{\cdot}25$ dB, $W = 0{\cdot}5$ dB. The 'worst case' values represent more practically available devices [2]; $X = -20$ dB, $L = 1$ dB, $W = 2$ dB. These figures are for the case of lithium niobate ($LiNbO_3$) directional coupler switches which, at the present time, are the most mature technology. However, the architectures can be realized with any $2 \times 2$ crosspoint technology, such as indium phosphide semiconductor laser amplifiers [3].

The attenuation calculations only consider the loss due to the directional couplers and fibre/substrate interfaces. No attempt is made to consider waveguide losses, or waveguide bends and crossovers. Interference effects [4] in the devices are also ignored; crosstalk is assumed to add to the signal linearly. The permissible values of SXR and $A$ are dependent on the application, so figures have been chosen to give some indication of the characteristics of switching systems. Thus, a minimum value of 11 dB is taken for the SXR since this represents the maximum noise level consistent with a Bit Error Rate (BER) of less than $10^{-9}$, assuming digital transmission. A generous maximum attenuation of 25 dB has been chosen; very few practical systems can accommodate a greater loss although this situation is changing with the proliferation in the use of optical amplifiers (see Table 1).

## 3. Crossbar switch

The crossbar switch is easily implemented optically. Figure 2 is an example of a $4 \times 4$ matrix utilizing 16

**Table 1. Restrictions on the switch size ($N$) for a number of architectures as a function of attenuation and crosstalk, assuming a SNR of 11 dB (for a BER of $10^{-9}$) and a maximum attenuation of 25 dB (PC = passive combiners; PS = passive splitters)**

| Architecture | Number of switches | Attenuation limit, best case | Atten. limit, worst case | Crosstalk limit, best case | Crosstalk limit, worst case |
|---|---|---|---|---|---|
| Crossbar | $N^2$ | 48 | 11 | 252 | 6 |
| Planar | $N(N-1)/2$ | 96 | 21 | 251 | 7 |
| Tree | $2N(N-1)$ | $7{\cdot}037 \times 10^{13}$ | 256 | $3{\cdot}584 \times 10^{239116}$ | $1{\cdot}042 \times 10^{239}$ |
| Tree, PS | $N(N-1)$ | 64 | 16 | $3{\cdot}619 \times 10^{75}$ | 128 |
| Double xbar | $2N^2$ | 95 | 20 | 794329 | 795 |
| Simp. tree | $N(5N/4-2)$ | $2{\cdot}815 \times 10^{17}$ | 2048 | $5{\cdot}884 \times 10^{238185}$ | $1{\cdot}644 \times 10^{209}$ |
| Simp. tree, PC | $N(3N/4-1)$ | 64 | 32 | 256 | 8 |
| Beneš | $N\log_2 N - N/2$ | $2{\cdot}815 \times 10^{14}$ | 2048 | $8{\cdot}507 \times 10^{37}$ | 16 |
| Dil. Beneš | $2N\log_2 N$ | $2{\cdot}815 \times 10^{14}$ | 1024 | $2{\cdot}228 \times 10^{189}$ | 1048576 |

directional couplers. In general, a $N \times N$ matrix uses $N^2$ switches, one for each crosspoint. The fabric is wide sense non-blocking but its control algorithm is very simple. When no connections are set up, all the switches are set to the cross state. To connect an idle input to an idle output, the switch that is connected to both is set into the bar state. To disconnect the call, the same switch is returned to the cross-state. The largest switch of this type that has been fabricated on a single substrate is an $8 \times 8$ on lithium niobate [5]. Polarization dependent $\Delta\beta$-reversal directional coupler switches were used operating at 1.3 μm. The interaction length of each coupler was 2 mm and the length of the whole device was 60 mm. The drive voltage for each switch was approximately 8 V. The worst extinction ratio on a switch was 18.6 dB. It seems unlikely that matrices larger than $16 \times 16$ will be possible on one substrate.

The minimum path length through the switch matrix is 1 (input $N$ to output 1) and the maximum is $2N-1$ switches (input 1 to output $N$). So the minimum value of $A$ is $L+2W$ and the maximum is $L(2N-1)+2W$. While this indicates that the attenuation through the matrix is not constant, the variation is not so marked as it appears since the attenuation is equalized to some extent by the varying lengths of waveguide required to reach the matrix from the edge of the substrate. In the $8 \times 8$ matrix mentioned earlier, the maximum attenuation was measured to be 6·8 dB, whilst the minimum was 5·3 dB [5].

The worst possible signal-to-crosstalk ratio occurs when a signal enters on input 1 and leaves on output 1, since the maximum number of other signals can pass through the switches that are used by the signal. Therefore, for $N=4$,

$$\mathrm{SXR} = -X - 10\log_{10} 3. \qquad (2)$$

For general $N$

$$\mathrm{SXR} = -X - 10\log_{10}(N-1). \qquad (3)$$

A more accurate formula, which takes attenuation into account, is [6]:

$$\mathrm{SXR} = X - NL - 10\log_{10}\left(\frac{1-10^{-(N-1)L/10}}{1-10^{-L/10}}\right). \qquad (4)$$

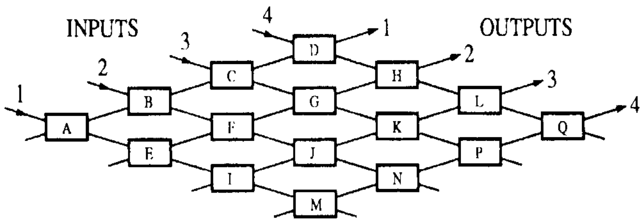


**Figure 2. A 4×4 optical crossbar switch.**

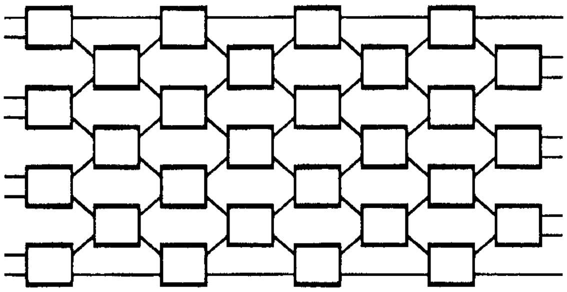

**Figure 3. An 8×8 planar network.**

On re-examining figure 2, switches IJMN are simply acting as one $2 \times 2$ switch and may be replaced by one switch reducing the number of switches required to $N^2-3$. The architecture is amenable to implementation in lithium niobate since no waveguide crossovers are necessary and the switches may be packed closely together.

## 4. Planar architectures

A planar rearrangeable switching network may be constructed frm $N(N-1)/2$ directional coupler switches [7], roughly half as many switches as for a classical crossbar. The penalty for the reduced number of switches is an increase in control complexity. A $8 \times 8$ rearrangeably non-blocking network is shown in figure 3, requiring eight stages. In general, a $N \times N$ network requires $N$ stages, where $N$ may be even or odd.

$N(N-1)/2$ is the minimum number of switches possible for a planar network. Assuming that the inputs and outputs are numbered 1 to $N$, starting from the top, to realize the assignment $i \rightarrow N+1-i$ each call must cross over every other call. There are $N(N-1)/2$ such pairs of calls and, given that no waveguide crossovers exist in a planar network, the number of switches cannot be less than $N(N-1)/2$. In the worst case, a call passes through $N$ switches, giving a SXR of

$$\mathrm{SXR} = -X - 10\log_{10} N, \qquad (5)$$

and the worst case attenuation is

$$A = LN + 2W, \qquad (6)$$

assuming implementation on one substrate. Since lithium niobate directional couplers are long, thin devices, their length limits the size of matrix that can be fabricated on one substrate. Figure 4 is a schematic of the way a matrix could be spread over several substrates. If the network has $2N-3$ stages, instead of $N$, it is self-routeing [8]; the state of a switch can be determined purely from the destinations of the calls entering it.

## 5. Tree architectures

Tree architectures [9] exhibit superior crosstalk performance for the architectures considered thus far, but at the expense of more crosspoints. For $N$ inputs and outputs, a crossbar needs $2N-1$ stages while a tree switch needs only $2\log_2 N$ stages allowing longer directional coupler switches for a given length of substrate, which in turn results in lower driving voltages. Tree architectures are realized through tree-structured splitters and combiners.

An 'active' $1\times N$ splitter (i.e. a demultiplexer) can be constructed from directional couplers; a $1\times 8$ splitter is shown in figure 5. In general, $N-1$ switches are required. An active combiner (i.e. a multiplexer) is simply a splitter in reverse. Only $\log_2 N$ signals are required to drive such a splitter or combiner since, in each stage, only one of the switches is used at once and hence one control signal can be shared by all. The largest device of this kind fabricated on one substrate is $1\times 16$ [10] using 15 $\Delta\beta$ reversal polarization independent switches operating at $\lambda = 1{\cdot}3\,\mu$m. The couplers were each 7 mm in length, the total device length being 50 mm. The insertion loss was 4·25 dB with a worst case crosstalk of 10 dB for a 70 V drive voltage. Larger architectures could be built by taking many one-substrate devices and cascading them; these will not be considered here.

Passive splitters and combiners can be made from fibre couplers or from Y-junctions in glass or silica-on-silicon integrated optics. If active splitters and combiners are used (figure 6) the resultant switch network is clearly strict-sense non-blocking using $2N(N-1)$ switches, nearly twice as many as the crossbar switch. The SXR is greatly improved over both the crossbar and planar architectures, since for a signal to find its way from an input to a wrong output, it must go to a wrong switch output and hence experience an attenuation of $X$, at least twice. The worst signal-to-crosstalk ratio is:

$$\mathrm{SXR} = -2X - 10\log_{10}(\log_2 N). \qquad (7)$$

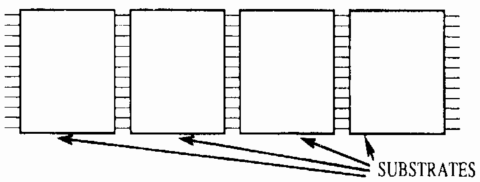


**Figure 4. A planar architecture spread over multiple substrates.**

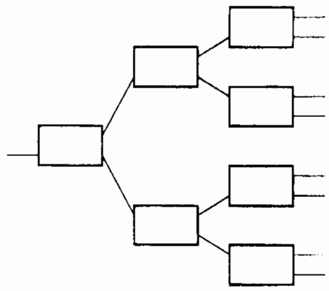

**Figure 5. An 1×8 active splitter.**

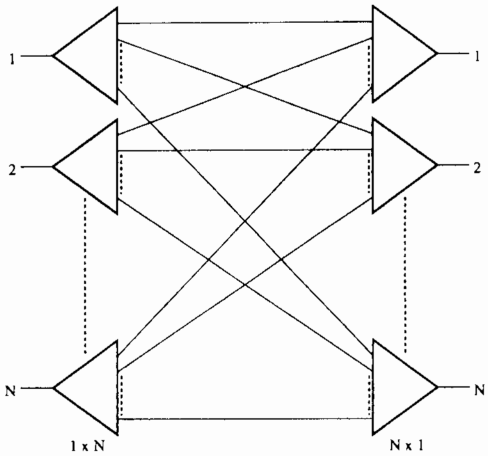


**Figure 6. The tree architecture.**

Assuming the splitters/combiners are fabricated on separate substrates the loss is

$$A \approx 2L\log_2 N + 4W, \qquad (8)$$

and on one substrate

$$A \approx 2L\log_2 N + 2W. \qquad (9)$$

A $4\times 4$ switch of this type, made from polarization independent $\Delta\beta$-reversal directional coupler switches at $\lambda = 1{\cdot}3\,\mu$m has been reported [11] (figure 7). The

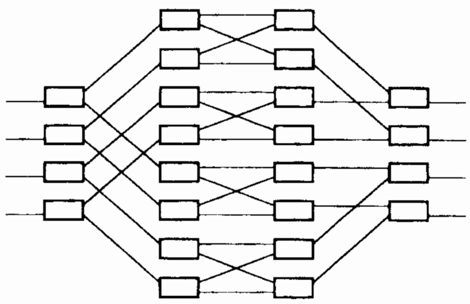

**Figure 7. A 4×4 tree structure.**

switch fabric was fabricated on one substrate of length ~50 mm. Each directional coupler was 4·3 mm long and required a switching voltage of 50 V. The SXR, based on measurement of individual switches was predicted to be greater than 58 dB. The attenuation was ~9.4 dB for the TM mode.

An alternative polarization independent 4 × 4 switch matrix has been realized [12] using 1 × 2 digital optical switches (DOSs) as opposed to directional coupler switches. DOSs do not require accurate control voltages and, when compared with directional couplers, are relatively wavelength insensitive. They do, however, require high drive voltages (±60 V) and exhibit high crosstalk levels, typically 10 dB for a single switch element. Crosstalk need not be a limiting problem for some applications, especially since it is reduced by the tree architecture. The switch was fabricated on one chip of length 52 mm, with an average insertion loss of 8·2 dB (for the TE polarization).

Another approach to realizing tree structures is to use passive splitters and active combiners allowing broadcast mode, where one input can be connected to more than one output. There is, however, the penalty of increased crosstalk and also increased attenuation due to the division of power in the splitters. The SXR is

$$\mathrm{SXR} \approx -X - 10\log_{10}(\log_2 N). \qquad (10)$$

Assuming the passive couplers have an excess loss of $L'$

$$A = (3 + L' + L)\log_2 N + 2W. \qquad (11)$$

It is also possible to have active splitters and passive combiners. The same formulae as above apply, although the geometry does not allow inputs to be broadcast to more than one output.

A polarization independent passive splitter/active combiner switch fabric has been fabricated on one substrate [13]; $\Delta\beta$-reversal switches were used operating at $\lambda = 1{\cdot}3\ \mu m$, requiring drive voltages ~4 V. The maximum attenuation was 13·9 dB and the crosstalk was measurement limited (< −35 dB). More recently a 16 × 16 switch was realized to act as the centre stage of a time division switching system [14]. Four passive splitters, or two active splitters, were placed on each substrate. The combiners were made up of 1 × 2 switches. The total insertion loss of the switch was 29 dB. The switching speed was better than 5 ns and the extinction ratio of each active combiner was better than 20 dB.

A 4 × 4 double crossbar switch is shown in figure 8 [15], an architecture related to the tree architecture (figure 6) since each row of four switches in the upper half of the network functions as an active splitter, and each row in the lower half is an active combiner. This fabric requires a large number of waveguide crossovers. The insertion loss assuming a single substrate is

$$A \approx (N + 1)L + 2W \qquad (12)$$

and the worst case crosstalk is

$$\mathrm{SXR} = -2X - 10\log_{10}(N - 1). \qquad (13)$$

This represents poorer performance since a signal can pass through up to $N$ switches in each combiner, rather than $\log_2 N$ in the original tree network. A 4 × 4 switch of this type has been fabricated using $\Delta\beta$-reversal directional couplers operating at 1·3 μm [15]. The SXR was 30 dB with no reported loss figure. The crosstalk at the numerous waveguide crossings was negligible since a large intersection angle (7°) was used. The substrate was 64 mm long, the crosspoints needing 8 V drivers.

## 6. Simplified tree structure

The simplified tree structure is a variant of the tree structure [16]. Considering figure 7, the switches in the centre two stages are divided into groups of four switches. Each of these groups functions as a 2 × 2 switch, and a single switch may be used to replace them, resulting in a simplified structure of figure 9. More generally, the simplified tree structure may be defined using the recursive definition of figure 10 [16]; the definition reduces a $2^i \times 2^i$ network to four $2^{i-1} \times 2^{i-1}$ networks and $2^{i+1}$ 2 × 2 switches. The reduction continues until $N = 4$, when directional coupler switches are substituted for the centre stage 2 × 2 switches. If the reduction is continued one stage further so that the centre stage switches are 1 × 1—no switch but just a link—the original tree network is produced.

The number of switches used is $N(5N/4 - 2)$ and the worst case SXR is

$$\mathrm{SXR} = -X - 10\log_{10}(1 + (\log_2 N - 1)x), \qquad (14)$$

where $x = 10^{X/10}$. Since the directional coupler switches in the centre stage are the only switches that can pass

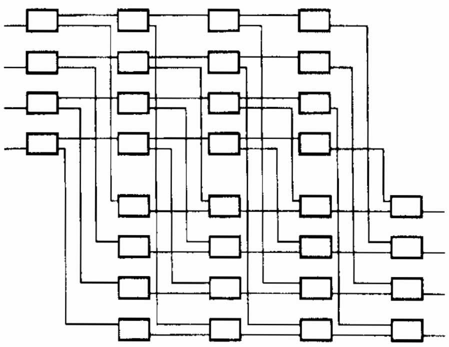

**Figure 8. A 4×4 double crossbar switch matrix.**

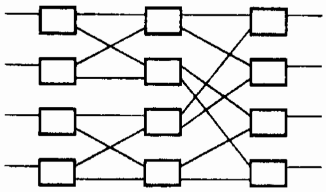

**Figure 9. A simplified tree structure, derived from a 4×4 tree structure.**

more than one signal at once, the SXR can be increased significantly by improving the extinction ratio of only these switches. The attenuation is (assuming one substrate):

$$A \approx (2 \log_2 N - 1)L + 2W. \tag{15}$$

The largest switch matrix of this type is a polarization independent 8×8 device [17] operating a 1.3 μm. The worst case insertion loss is 12 dB and the worst case SXR is 18·7 dB. 64 directional couplers were used, each 5·7 mm in length with a 85 V switching voltage. The device was 65 mm long.

Another approach is to use 2×1 passive couplers instead of directional couplers in the rightmost stage of figure 10. This reduces the number of switches used while reducing the SXR $N(3N/4-1)$ switches are used and the worst case SXR is [16]:

$$\mathrm{SXR} = -X - 10 \log_{10}(N/2). \tag{16}$$

The total loss is now

$$A = (\log_2 N)L + (\log_2 N - 1)(L' + 3) + 2W. \tag{17}$$

As 8×8 device has been realized [18] comprising 40 polarization independent Δβ-reversal directional couplers and 24 passive combiners. Each switch was 9 mm long, giving a total device length of 61 mm. The reported switching voltage was 11 V, the worst case SXR 13 dB and the total attenuation was 20 dB.

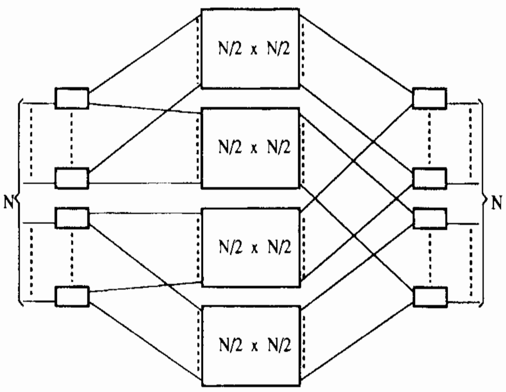


**Figure 10. Recursive definition of the simplified tree architecture.**

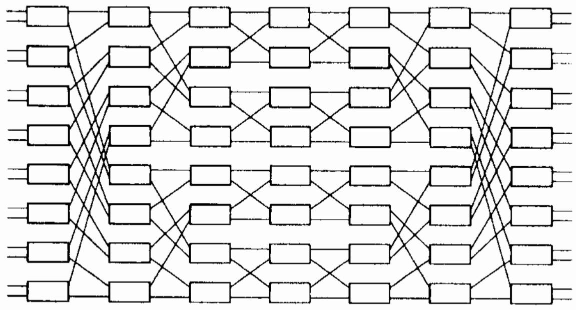

**Figure 11. A 16×16 Beneš network.**

## 7. Beneš and dilated Beneš networks

Optical switching architectures are often quite different from their classical electronic counterparts. However, the Beneš network, a rearrangeably non-blocking architecture, lends itself easily to implementation with directional couplers, since it grows recursively from 2×2 elements. A $N \times N$ Beneš network consists of $2 \log_2 (N-1)$ stages of $N/2$ switches [19].

A 16×16 polarization dependent Beneš network [20] (figure 11) has been fabricated in a substrate of length 70 mm and operates at 1·3 μm using reversal switches throughout. Due to the nature of the architecture, a substantial amount of the substrate length was utilized by waveguide crossovers (minimum acceptable angle 7°) and waveguide bends (minimum acceptable radius 35 mm). Consequently, the electrode length on the switches was only 2 mm, giving a relatively high switching voltage of 40–50 V. Individual switch elements had crosstalk better than −20 dB, crossovers had crosstalk better than −25 dB.

The theoretical attenuation for this type of network is:

$$A = (2 \log_2 N - 1)L + 2W, \tag{18}$$

and the SXR is:

$$\mathrm{SXR} = -X - 10 \log_{10}(2 \log_2 N - 1), \tag{19}$$

since each signal passes through $2 \log_2 N - 1$ switches.

To reduce the crosstalk level further, the Beneš network can be dilated [21], reducing the crosstalk (by ensuring, at most one call traverses any switch at once)

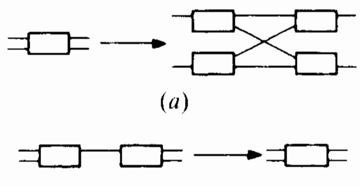


**Figure 12. (a) First step in dilation; (b) second step in dilation.**

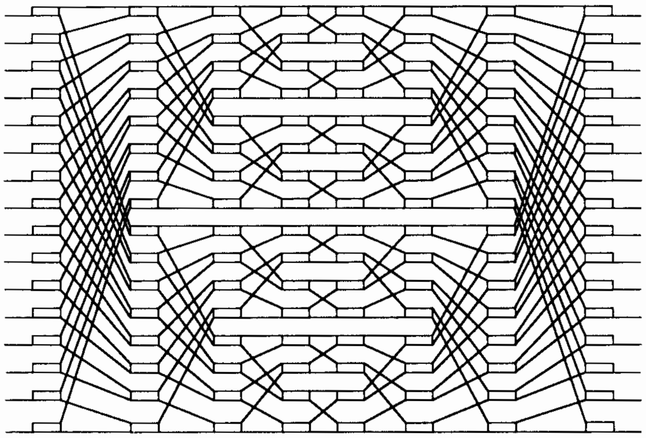

**Figure 13. A 16 × 16 dilated Beneš network.**

at the expense of roughly doubling the number of switches. To make a dilated Beneš network from a regular Beneš network, first replace each switch with a four-swtich structure of figure 12(*a*), which ensures that only one call goes through each switch and, while still conserving this condition, pairs of back-to-back switches may be connected (figure 12(*b*)).

A 16 × 16 dilated Beneš network (figure 13) is very similar in appearance to an ordinary 32 × 32 Beneš network, but with two differences. Each input switch has only one input used and each output switch has only one output used and, secondly, the centre stage is missing. Any assignment of inputs into outputs can be realized while only having one signal passing through each switch, drastically reducing crosstalk [21]. The control algorithm is very similar to that of a conventional Beneš network. The attenuation is:

$$A = 2L \log_2 N + 2W, \qquad (20)$$

and the crosstalk is given (approximately) by:

$$\mathrm{SXR} = -2X - 20 \log_{10} (2 \log_2 N - 1) + 3. \qquad (21)$$

The SXR figure is over twice as great as for a conventional Beneš network.

A polarization dependent 16 × 16 dilated Beneš network (figure 13) has been realized in lithium niobate using $\Delta\beta$ reversal directional couplers [22]. To allow lower drive voltages through longer electrodes (average 12·4 V for 6·2 mm length) the fabric was made on two substrates, each 90 mm long. The insertion loss was 12·4 dB, and the extinction ratios of individual switches are all better than 15 dB, and most better than −20 dB, indicating that the SXR of the whole fabric is always better than 20 dB. The best case switching time was 1 ns and the worst case was 2·5 ns allowing the switch to be used for TDM switching [23] where the space switch must be reconfigured every timeslot. The worst case of 2·5 ns could be reduced to 1 ns by proper design of the electrode lead pick up to eliminate unnecessary capacitance.

## 8. Extended generalized shuffle networks

Extended generalized shuffle (EGS) networks [24] are an extended class of architectures, which includes many

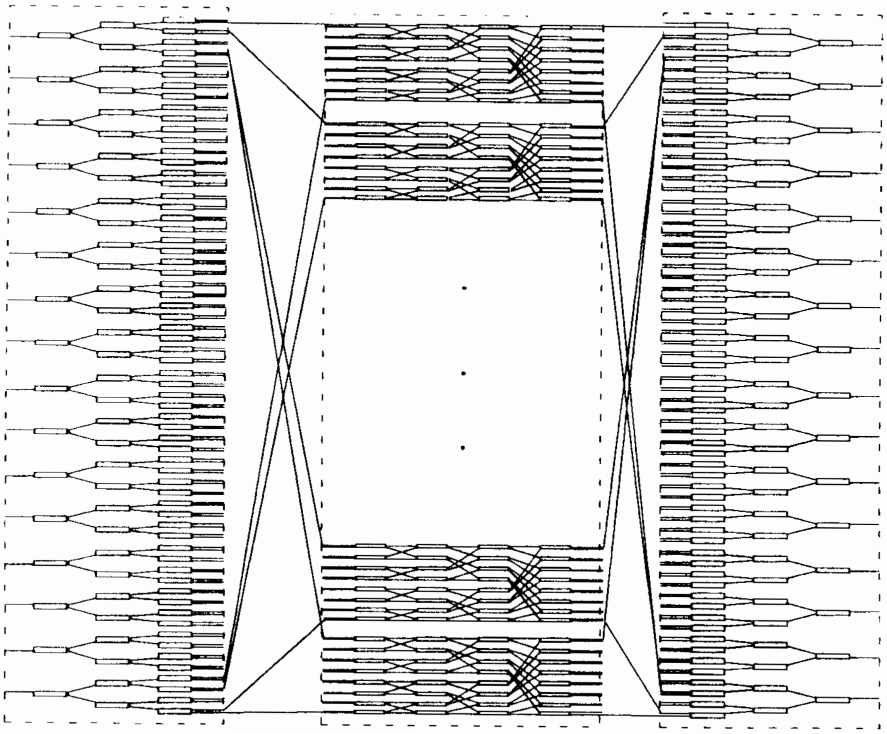

**Figure 14. A 16 × 16 extended generalized shuffle network architecture.**

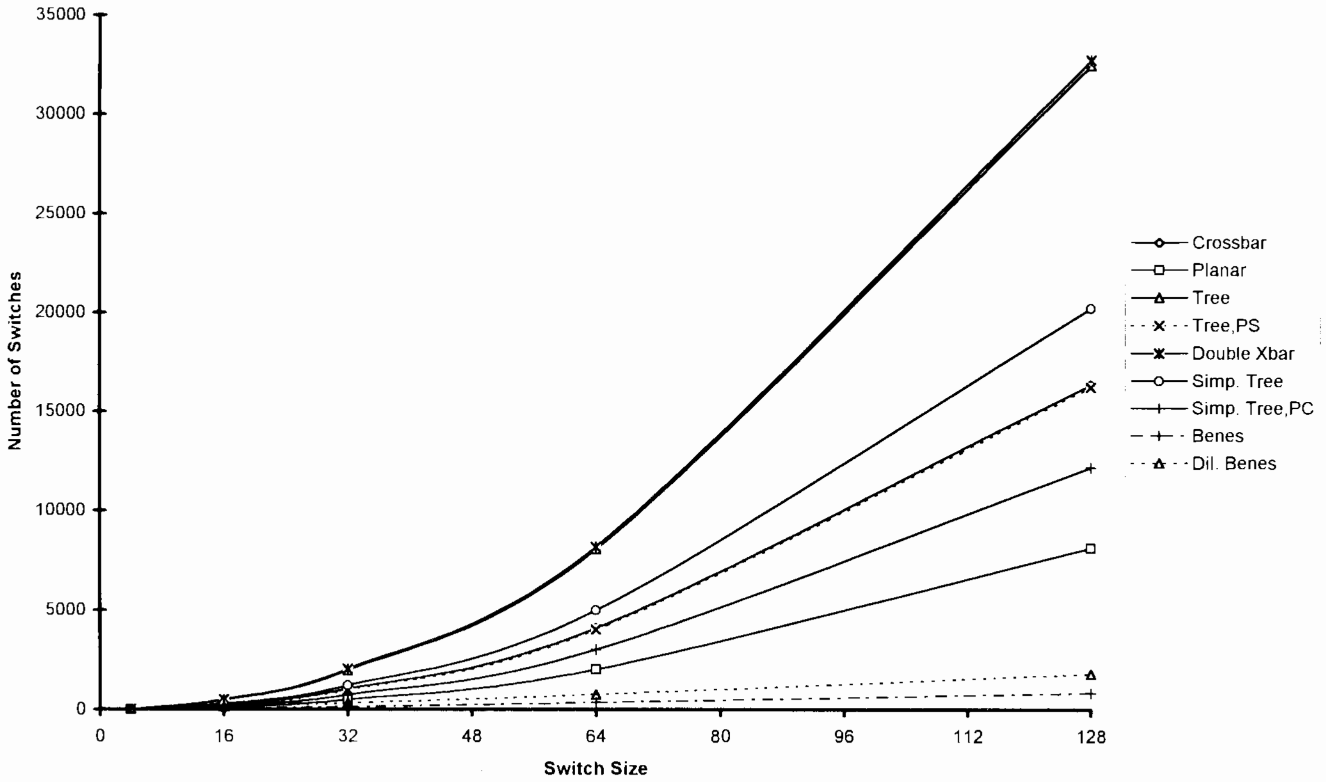


**Figure 15. The number of switches required as a function of switch size ($N$) for a number of architectures.**

existing networks as special cases. A dilated EGS switch has been implemented (figure 14) [25], which has 16 inputs and outputs and consists of 448 directional couplers on 23 substrates, which are polarization sensitive and hence interconnected by polarization preserving fibre. The architecture is strict-sense non-blocking. Crosstalk in the fabric outputs is always below −25 dB, and loss varies from −17·9 to −26·5 dB with 97% of the results falling in a 6 dB range.

## 9. Conclusions

A number of optical guided-wave space-switch architectures has been reviewed. Table 1 summarizes the characteristics of these fabrics, their application sectors being driven by the combination of, and trade-offs that exist between, the parameters. Figures 15–17 show their behaviour with respect to number of switches, attenuation and crosstalk as a function of switch size (number of inputs $N$). In their calculations, the formu-

**Table 2. Architectures listed in order of merit for various performance characteristics. (PC = passive combiners; PS = passive splitters; dashes indicate no preference)**

| Crosspoint count | Attenuation | Crosstalk | Control complexity |
|---|---|---|---|
| Beneš | Simplified tree | Tree | — |
| Dilated Beneš | Tree | Simplified tree | — |
| Planar | Beneš | Dilated Beneš | — |
| Simp. tree, PC | Dilated Beneš | Tree, PS | — |
| Tree, PS | Planar | Beneš | — |
| Crossbar | Double crossbar | Double crossbar | — |
| Simplified tree | Simp. tree, PC | Simp. tree, PC | Beneš |
| Tree | Tree, PS | Crossbar | Dilated Beneš |
| Double crossbar | Crossbar | Planar | Planar |

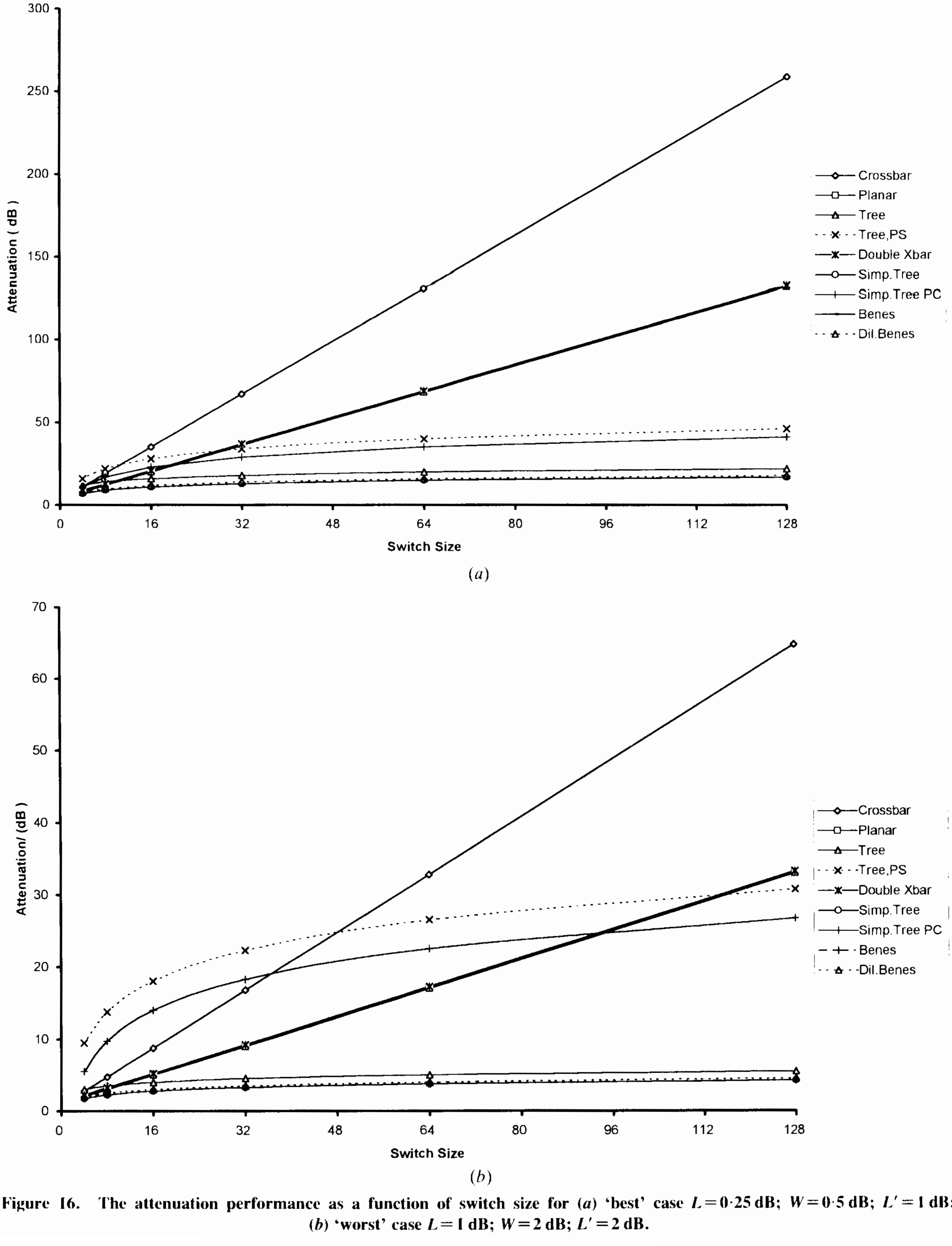


(*a*)



(*b*)

**Figure 16. The attenuation performance as a function of switch size for (*a*) 'best' case $L=0{\cdot}25$ dB; $W=0{\cdot}5$ dB; $L'=1$ dB; (*b*) 'worst' case $L=1$ dB; $W=2$ dB; $L'=2$ dB.**

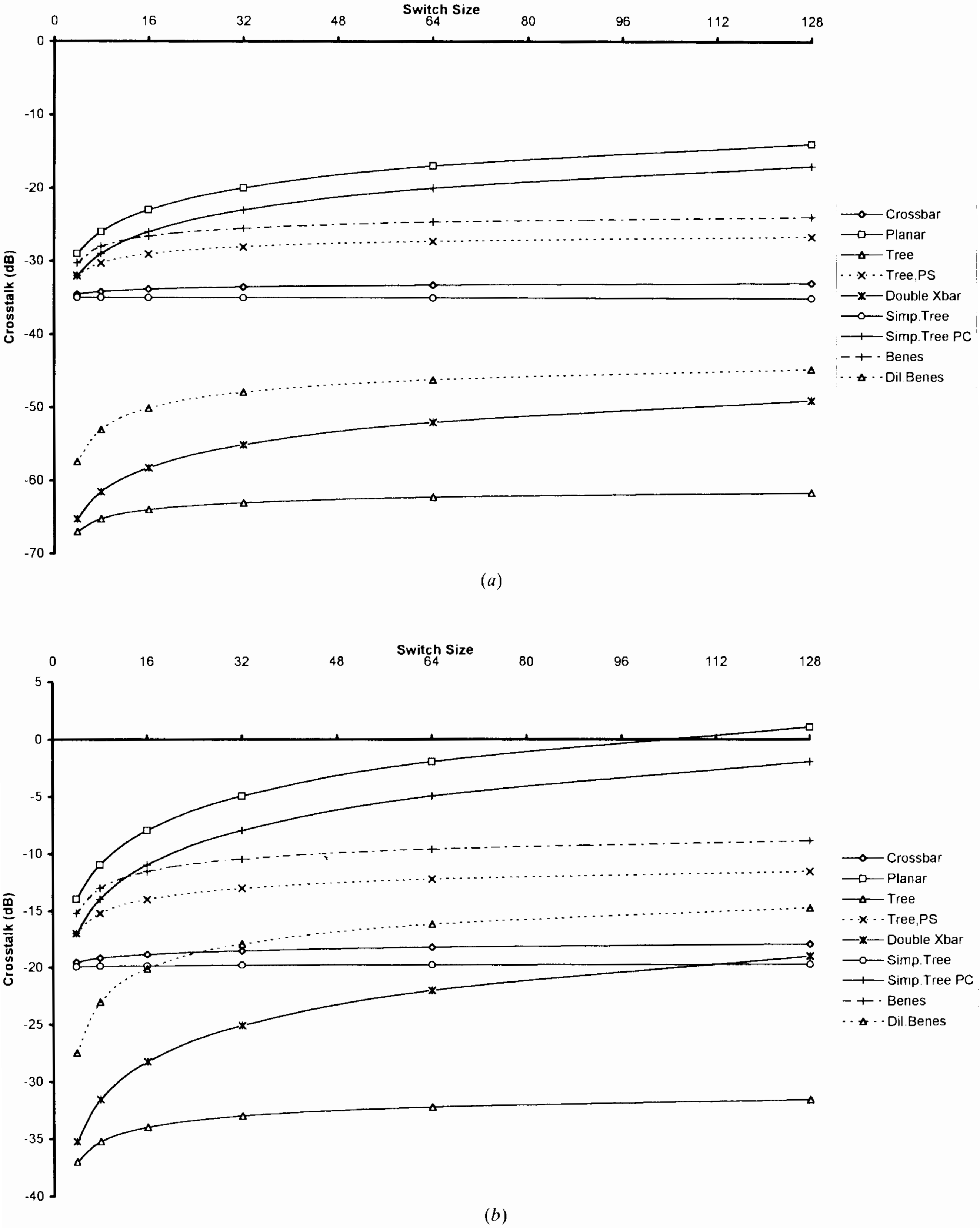


**Figure 17.** The crosstalk performance as a function of switch size for (*a*) 'best' case $X = -35$ dB; (*b*) 'worst' case $X = 20$ dB.

lae presented in the paper—rather than experimental results—are used in order that a meaningful comparison can be made.

The figures further highlight the trade-offs between different parameters. For example, networks using more switches, generally, have superior attenuation, crosstalk and/or control complexity. To accentuate this, Table 2 arranges the architectures into lists for different performance criteria, the best architectures being at the top of the relevant list. Inspection of the table reveals that no single architecture appears at the top of all four lists.

To date, the most notable application of a guided-wave optical switch fabric has been as a node in an optical transport layer, based on a multiwavelength implementation [26], and used as an overlay on top of the existing telecommunications network. Similar implementations have been researched worldwide [27].

## References


[1] Selvarajan, A., and Midwinter, J. E., 1989, *Opt. & Quant. Elect.* **21**, 1–15.
[2] Spanke, R. A., 1987, *IEEE Comm Mag.*, 42–48.
[3] Sherlock, G., Burton, J. D., Fiddyment, P. J., Sully, P. C., Kelly, A. E., and Robertson, M. J., 1994, *Electron Lett.*, 137–138.
[4] Legg, P. J., Hunter, D. K., Andonovic, I., and Barnsley, P. E., *IEEE Phot. Technol. Lett.*, **6**, 661–663.
[5] Granestrand, P., Stoltz, B., Thylen, L., Bergvall, K., Dolissen, W., Heinrich, H., and Hoffman, D., 1986, *Electron. Lett.*, 816–818.
[6] Hinton, H. S., 1984, *Proc. GlobeCom.*, 26.5.1–26.5.5.
[7] Spanke, R. A., Benes, V. E., 1987, *Appl. Opt.*, **26**, 1226–1229.
[8] Obara, H., Okamato, S., Vanatsu, H., and Matsunaga, H., 1990, *Electron. Lett.*, **26**, 520–521.
[9] Spanke, R. A., 1986, *IEEE J. Quant. Electron.*, **22**, 964–967.
[10] Watson, J. E., Milbrodt, M. A., and Rice, T. C., 1986, *J. Lightwave Technol.*, 4, 1717–1721.
[11] Granestrand, P., Lagerstrom, B., Svensson, P., and Thylen, L., 1988, *Electron. Lett.*, **24**, 1198–1200.
[12] Granestrand, P., Lagerstrom, B., Svensson, P., Thylen, L., Stoltz, B., Bergvall, K., Falk, J. E., and Olofsson, H., 1990, *Electron. Lett.*, **26**, 4–5.
[13] Bogert, G. A., 1987, *Proc. Topical Meeting on Photonic Switching*, Incline Village.
[14] Burnett, I. M., and O'Donnell, A. C., 1990, *EFOC/LAN*, Munich.
[15] Kondo, M., Takudo, N., Komatsu K., and Ohta, Y., 1985, *IOOC/ECOC*, Venice, pp. 361–364.
[16] Okagam H., Matoba, A., Shibuga, R., and Ishido, T., 1990, *J. Lightwave Technol.*, **7**, 1023–1028.
[17] Nishimoto, H., Iwasaki, M., Suzuki, S., and Kondo, M., 1990, *IEEE Phot. Technol. Lett.*, **2**, 634–636.
[18] Matoba, A., Okayama, H., Shibuga, R., and Ishida, T., 1989, *Electron. Lett.*, **25**, 165–166.
[19] Benes, V. E., 1965, *Mathematical Theory of Connecting Networks and Telephone Traffic*, Academic Press.
[20] Duthie, P. J., Wale, M. J., and Bennion, I., 1990, *Tech. Digist Int. Topical Meeting on Photonic Switching*, Incline Village.
[21] Padmanabhan, K., and Netravali, A. N., 1987, *IEEE Trans. Comm.*, **35**, 1357–1365.
[22] Murphy T. Q., Kemmerer, C. T., and Moser, D. T., 1991, *Topical Meeting on Photonic Switching*, paper PD3, Salt Lake City.
[23] Thompson, R. A., Horenkomp, J. J., Bergland, G. D., 1990, *13th Int. Switch. Symp.*, Stockholm.
[24] Richards, G. W., 1993, *INFOCOM*.
[25] Bergstein, S. S., and Ambrose, A. F., 1993, *OFC*, paper PD30.
[26] Hill, G. R., Chidgey, P. J., Kaufold, F., Lynch, T., Sahlen, O., Gustavsson, M., Janson, M., Lagerstrom, B., Grasso, G., Meli, F., Johansson, S., Ingers, J., Fernandez, L., Rotolo, S., Antonielli, A., Tebaldini, S., Vezzoni, E., Caddedu, R., Caponio, N., Testa, F., Scavennea, A., O'Mahony, M. J., Zhou, J., Yu, A., Sohler, W., Rust, U., and Hermann, H., 1993, *J. Lightware Technol.*, **11**, 667–679.
[27] Sato, K.-I., Okamato, S., and Hadama, H., 1994, *IEEE J. Select. Areas Comms.*, **12**, 159–170.